Enhancement of osteoprogenitor cell response on titanium by helium atmospheric pressure glow discharge treatment

Barbora Vagaska

Department of Medical Science
The Graduate School, Yonsei University

Enhancement of osteoprogenitor cell response on titanium by helium atmospheric pressure glow discharge treatment

Directed by Professor Jong-Chul Park

The Master's Thesis
submitted to the Department of Medical Science,
the Graduate School of Yonsei University
in partial fulfillment of the requirements for the degree
of Master of Medical Science

Barbora Vagaska

June 2010

This certifies that the Master's Thesis
of Barbora Vagaska is approved.

---------- ----------

Thesis supervisor: Jong-Chul PARK

Jin Woo LEE

Hyeong Cheol YANG

The Graduate School
Yonsei University

June 2010

Acknowledgements

I would like to express my thanks to all the people who have helped and supported me during my studies in the exciting and beautiful Korea.

First and foremost I would like to give my sincerest gratitude to my supervisor prof. Park Jong-chul for all the guidance and support during my studies at Yonsei University. Prof. Park is very open-minded and willing to help his students in their research. Thanks to his help and very generous support in all areas, my research life in Korea was a very rewarding experience.

I also gratefully acknowledge the second supervisor of this thesis, Han Inho, for his crucial contribution, advice and supervision especially in the area of material science and plasma treatment. Without his innovative ideas this research and so also this thesis would not be possible. I appreciate also the guidance and suggestions of the members of my thesis committee prof. Lee Jin Woo and prof. Yang Hyeong Cheol.

In my daily work I have been blessed with a friendly and cheerful group of fellow students and lab colleagues. In the beginning it was not easy for a foreigner like me, who could barely speak the language to fit in a fully Korean environment, but I would really like to thank them all for being so patient, friendly and helpful to me. 감사합니다.

I appreciate also the generous support from the Korean government and NIIED organization who granted me the KGSP scholarship. Without this support my dream to study at a graduate school in Korea would simply not be possible.

And finally, my greatest thanks goes to my family, my parents Marta and Dušan, who endlessly continued to support me with love and patience in all of my studies and always trusted me in my life decisions, no matter how unconventional or crazy they were. Ďakujem.

Barbora Vagaská

Seoul, June 2010

TABLE OF CONTENTS

LIST OF FIGURES

LIST OF TABLES

Abbreviations

He-APGD: helium atmospheric pressure glow discharge

UV: ultra violet irradiation

ECM: extracellular matrix

XPS: X-ray spectroscopy

SEM: scanning electron microscopy

AFM: atomic force microscopy

MSC: mesenchymal stem cells

DPC: dental pulp cells

PBS: phosphate buffer saline

α-MEM: minimum essential medium-alpha modification

DMEM: Dulbecco's modified Eagle's medium

FBS: fetal bovine serum

BSA: bovine serum albumin

FN: fibronectin

MTT: 3-(4,5-dimethylthiazol-2-yl)-diphenyltetrazolium bromide

ALP: alkaline phosphatase

Abstract

Enhancement of osteoprogenitor cell response on titanium by helium atmospheric pressure glow discharge treatment

Barbora Vagaska

Department of Medical Science

The Graduate School,Yonsei University

(Directed by Professor Jong-Chul Park)

Titanium and its alloys are widely used in dental or orthopedic implants, thanks to their excellent mechanical properties and high biocompatibility. The current approach in biomaterial design is to induce in situ regeneration of bone tissue and thus improve integration of the implants and reduce their failure. This study examines helium atmospheric pressure glow discharge (He-APGD) treatment as a method of surface modification for improving osteoinductive properties of titanium. He-APGD treatment effectively modified the titanium surfaces, by rapidly cleansing the surface contaminants and creating highly hydrophilic surface. The effect of plasma treatment of titanium on the initial phase of cell response to biomaterial was examined. A significantly higher fibronectin adsorption, followed by enhanced adhesion,

spreading and proliferation of osteoblast progenitor cells (MC3T3-E1, mouse pre-osteoblasts and primary cultures of human mesenchymal stem cells and dental pulp stem cells) was observed on plasma treated titanium in comparison with the non-treated control. Moreover, this positive effect seemed to increase gradually with the increasing plasma treatment time. These *in vitro* results demonstrate that He-APGD treatment is an effective and promising method of surface modification for improving titanium bioactivity.

Key words: titanium, atmospheric pressure glow discharge, osteoblast, mesenchymal stem cells, dental pulp cells, cell-biomaterial interaction

Enhancement of osteoprogenitor cell response on titanium by helium atmospheric pressure glow discharge treatment

Barbora Vagaska

Department of Medical Science

The Graduate School,Yonsei University

(Directed by Professor Jong-Chul Park)

I. INTRODUCTION

1. Titanium biomaterials

Biomaterials used in bone implants need to have sufficient mechanical strength and firm structure because they need to be able to bear the weight load. Titanium and its alloys have been widely used in dental or orthopedic implants, especially thanks to their resistance to corrosion and inertness in biological fluids, which renders them high biocompatibility. They also have superior mechanical properties, such as high specific strength to sustain cyclic loading, high wear resistance to minimize debris formation and low elastic modulus, which decreases the risk of bone resorption around the implant[1, 2]. However, their inertness is also the major drawback. At one hand it helps to avoid adverse tissue reactions upon implantation;

on the other hand it is the main reason of encapsulation of the implant into a fibrous tissue and leads ultimately to its failure.

Therefore, modern advanced materials should not only be biocompatible, but they are specifically designed to be "bioactive"[3]. This means they should elicit specific desired cellular responses, such as cell adhesion, proliferation and differentiation into a specific cell type, i.e. bone cells (osteoinduction) that will form a new bone and thus integrate the implant strongly into the surrounding natural tissue (osteoconduction)[4].

It is well-established that these processes depend mainly on surface properties of the materials that are usually very different from their bulk properties[5]. Therefore the research has focused on various surface modifications that could control and enhance the response of osteoblastic cells.

2. Surface modifications of titanium

The modification methods can be divided into three major groups: mechanical, involving physical treatment, shaping or removal of the materials surface (e.g. blasting, machining); chemical, involving chemical reaction at the interface between titanium and a solution (e.g. acidic/alkaline treatment, anodic oxidation); and physical methods, where surface modification can be attributed to electrical, thermal or kinetic energy (e.g. plasma spraying, sputtering, ion implantation)[6]. Surface treatments induce two basic changes on the titanium surface: changes in surface morphology and changes in surface chemistry. Even though these methods were successful in enhancing the osteoblast responses and osseointegration

to a certain level, they also have some major drawbacks[7, 8]. Despite of a certain recent stagnation in this area of research, two new and promising methods have been introduced. They both aim on creating and preserving highly hydrophilic surfaces.

First, is a method of preserving fresh and active surface created by combination of sand blasting and acid-etching (SLA) in oxygen free environment by immersion in isotonic sodium chloride solution. The titanium surface is protected from contaminants from atmosphere and preserves high surface energy, which was shown to have a positive effect on cell activity and differentiation, as well as on bone anchorage of implants[9-11]. The second method is using ultraviolet (UV) irradiation to create a superhydrophilic surface, which enhanced osteoblastic cell attachment, proliferation, and differentiation[12, 13]. This relatively simple and effective surface modification has a major disadvantage in requirement of a long treatment time (24 hr) which makes it very impractical and problematic to implement into praxis.

3. Gaseous plasma discharge (glow discharge)

Recently there has been also a great interest in surface modifications of biomaterials by plasma treatment. Glow discharge plasma is a low-temperature, low pressure gas in which ionization is controlled by energetic electrons. During the treatment, the surfaces exposed to the plasma are bombarded by electrons, ions, photons and other charged particles. Glow discharge plasma treatments have been widely used especially for cleansing and surface processing in microelectronics industry[14]. In the biomaterials field it was used as a sterilization or cleansing method.

It is also very well established in modification of polymer surfaces, for increasing their surface energy, producing thin polymer coatings, inducing polymerization and grafting of chemical groups[15, 16].

Most of the applications in biomaterial surface modifications have used plasma equipments that are operated at vacuum pressure, requiring complicated and expensive vacuum systems for operation. The operation pressure of glow discharge has an effect on the discharge stability, population, and kinetic energy of the excited species[17, 18]. At high operation pressure, such as atmospheric pressure, the discharge molecules have a decreased mean free path, and because of higher rate of collisions their kinetic energy decreases. These limitations can be overcome through the use of high voltage power supply, reduced electrode distance, and use of appropriate plasma processing gases. Under these conditions, the discharge is able to sustain a large population of excited species. Higher population of high energy particles makes the treatment with plasma more effective and requires less time. Moreover, thanks to its relatively easier and cheaper operation in comparison with the vacuum systems it becomes a promising method also for biomaterial surface modifications.

4. **Plasma treatment of titanium**

Event though enhancement of cellular responses on plasma treated polymers has been well documented; there are relatively very few studies that examine the effect of plasma treatment on metallic biomaterials such as titanium. A few studies have reported that plasma treatment had a cleansing effect[19], enhanced surface energy and protein adsorption[20], or even adhesion of osteoblast-like cells[21]. However,

the used plasma treatment systems differ from each other and operate under vacuum conditions.

The main problem of applying atmospheric pressure glow discharge to metals is formation of arcs in the discharge spaces. Arc development on electro-conductive materials in a high electric field can be successfully prevented by using a duty controlled pulse electric waveform to cut off the electrical energy inducing time and using helium as a processing gas to obtain a lower processing voltage. Moreover, during atmospheric pressure glow discharge helium excites hydroxyl groups[22], which may be then grafted onto the excited surface and additionally increase the surface hydrophilicity.

5. Objectives of the study

The aim of this study is to evaluate whether surface modification of titanium with helium atmospheric pressure glow discharge (He-APGD) can enhance its bioactivity in *in vitro*. Using the murine cell line of pre-osteoblasts (MC3T3-E1, clone 4), as well as primary cultures of human mesenchymal stem cells (MSC) and human dental pulp cells (DPC), the ability of the plasma treatment to stimulate initial cell adhesion, proliferation and osteogenic differentiation was examined. Physicochemical characterization and protein adsorption to the samples was examined to explore the effects of the plasma treatment on the titanium surface as well as the underlying mechanism on cell response.

II. Materials and Methods

1. Titanium

Titanium samples were prepared from grade II titanium sheets (CP-2, thickness 0.3 mm) in a shape of disks (diameter 13 or 20 mm). Before the plasma treatment they were ultra-sonically cleansed consecutively in acetone, ethanol and de-ionized water for 8 min and then blow-dried with clean air.

2. Plasma treatment

He-APGD treatment unit was assembled as shown in Figure 1. Head unit was made of two alumina plates (thickness 1 mm) as dielectric barriers. Distance between the plates was 1 mm and the sample was placed between them. After sealing the dielectric barriers, working gas (helium) was introduced into the narrow space between them at a rate of 200 ml/min. Aluminum electrodes were installed on the outer side of the alumina plates and a high voltage pulse bipolar power supply (HPI500, FT-Lab Co., Korea) was employed as energy source to fire plasma. The applied voltage, frequency and duty were 2.0 kV, 20 kHz and 20%, respectively. Treatment time was set to 3 s, 4 min and 8 min and non-treated disks (0 s) were used as control.

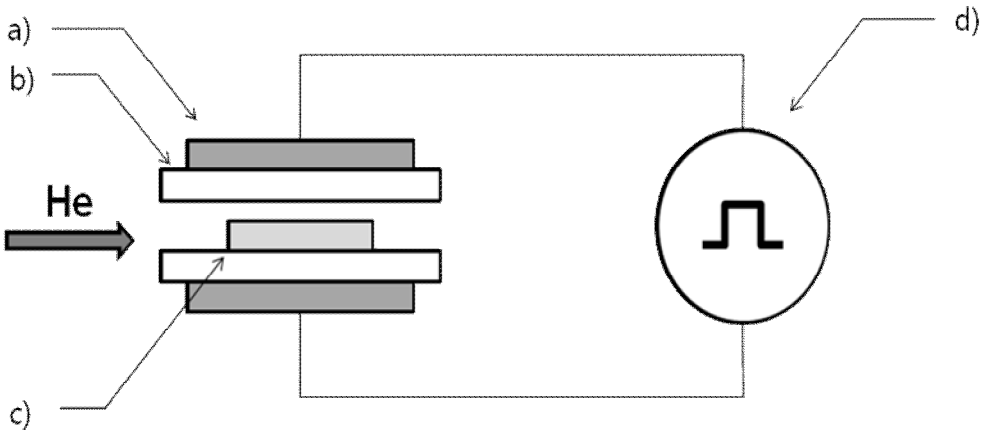

Figure 1. Diagram of He-APGD system. a) aluminum electrode, b) dielectric barrier, c) sample - Ti disk and d) bipolar type high voltage power supply.

3. Physico-chemical characterization of samples

A. X-ray photoelectron spectroscopy

Changes in surface chemistry of titanium by He-APGD treatment were surveyed with X-ray photoelectron spectroscopy (XPS, ESCA Lab 220i-XL, VG Sci. Inst., USA). In order to observe the surface chemistry, ion-beam etching process was not performed.

B. Water contact angle measurements

Changes in surface wettability were evaluated by measuring water contact angle using sessile drop method. De-ionized water (8 µl) was dropped from the tip of needle which was placed 8 mm high from specimen top surface. The pictures were taken by Nikon D80 camera equipped with 65 mm ED lens and 5 times magnification filter (Nikon, Japan). Water contact angle was measured from these pictures by Image J software (NIH, USA).

Wettability restoration was observed by water contact angle measurements on determined dates, over a period of 4 weeks. After the He-APGD treatment the disks were stored in dark at 4°C.

C. Scanning electron microscopy and atomic force microscopy

Surface morphologies of titanium before and after the He-APGD treatment were observed with scanning electron microscopy (Fe-SEM, S-4200, Hitachi, Japan).

Surface roughness and 3D topography was examined by atomic force microscopy (AFM, Autoprobe CP, Park Scientific Instruments, PSI). The AFM images and roughness parameters were obtained from scans of area 0.5 µm × 0.5 µm in contact mode at scanning rate 1 Hz, using Si tips with a tip radius of ~ 10 nm.

4. Protein adsorption

Fetal bovine serum (FBS, WelGENE Inc, Korea), bovine serum albumin (BSA, 1 mg/ml in PBS, Invitrogen, USA) and bovine plasma fibronectin (FN, 100 µg/ml in PBS, Sigma) were used as model proteins to study protein adsorption to the titanium surfaces.

A. Micro bicinchoninic acid assay

Protein solution was pipetted on the top of the samples in 24-well plate to completely cover the surface (200 µl/well) and then incubated for 1 hr at 37°C in 5% CO_2 atmosphere incubator. In order to remove the non-adherent protein the samples were rinsed twice with phosphate buffered saline (PBS, WelGENE). Then the samples were moved to a new well plate and incubated with 200 µl/well of 2% (w/v) sodium dodecylsulphate (SDS, Sigma) for 48 hr at room temperature with shaking. The amount of eluted proteins in the SDS solution was determined by micro bicinchoninic acid assay (BCA, Thermo Scientific, Pierce Biotechnology, IL, USA) according to the modified protocol for 96-well plate as provided by the manufacturer.

B. Fibronectin adsorption - ELISA

Adsorption of fibronectin was evaluated also by a modified ELISA method. He-APGD treated and control disks were placed in 24-well plate, loaded with 200 µl of either FN solution (25 µg/ml in PBS) or FBS and incubated for 1 hr at 37°C in 5% CO_2 atmosphere incubator. After washing the samples with PBS two times, they were blocked with 5% (w/v) BSA solution for 30 min at 37°C and then incubated with monoclonal anti-fibronectin antibody overnight at 4°C (dilution

1:1000, Takara Bio Inc., Shiga, Japan). After washing three times with PBS the samples were immersed for 1 hr in secondary antibody solution (goat anti-mouse IgG conjugated with alkaline phosphatase, dilution 1:2000, Sigma). Colorimetric detection was performed by incubation of the samples with phosphatase substrate, p-nitrophenyl phosphate (pNPP, Sigma), which is converted to a yellow, soluble end product. The disks were topped with 10 mM pNPP solution in glycine buffer (0.1 M glycine with 1 mM $MgCl_2$ and 1 mM $ZnCl_2$, pH 10.4) and incubated at 37°C for 30 min. Finally, absorbance of the product at 405 nm was measured spectrophotometrically.

5. Cell culture

MC3T3-E1 mouse pre-osteoblast cells (Riken, Japan) were maintained in minimum essential medium α - modification without ascorbic acid supplemented with 10% fetal bovine serum and 1% antibiotic antimycotic solution (α-MEM, all from WelGENE).

Primary culture of human mesenchymal stem cells was maintained in mesenchymal stem cell Basal Media (MSC Basal Media) supplemented with mesenchymal stem cell growth medium (MSCGM) Single Quots (Lonza, USA).

Dental pulp cells were a kind gift from Dr. Yu-Shik Hwang from Kyung Hee University, Seoul, Korea. The DPC cells are primary culture of stem cells which share many common features with bone marrow stem cells were isolated from the pulp of human third molars after receiving the informed consent

from patients. The cells were cultured in Dulbecco's modified Eagle's medium (DMEM) supplemented with 10% FBS and 1% of penicillin streptomycin solution (WelGENE).

Primary cultures were used up to 10^{th} passage and MC3T3-E1 cells up to 15^{th} passage for all experiments. Cells were grown at 37°C in 5 % CO_2 atmosphere incubator.

Before the cell seeding titanium disks were always sterilized by 30 min incubation in 70 % (v/v) ethanol and then washed twice in distilled water.

6. Cell adhesion - MTT assay

Cell attachment was determined at 2-6 hr after seeding according to the cell type using MTT assay. Briefly, cells were seeded at the initial density of 3.0×10^4 cells/cm^2 and incubated for 2-6 hr in a CO_2 atmosphere incubator. Then, the unattached cells were removed by gentle washing with PBS, the samples were carefully moved to a new well plate and incubated with 3-(4,5-dimethylthiazol-2-yl)-diphenyltetrazolium bromide (MTT, final concentration 0.5 mg/ml, Amresco, Solon, OH, USA) for 2 hr. The formed formazan salts were dissolved in dimethyl sulfoxide (DMSO) and the optical density measured at wavelength of 570 nm by spectrophotometer.

7. Cell morphology

A. Cell attachment area

For cell morphometric analysis cells were seeded at the initial seeding density of 5.0×10^3 cells/cm^2 and after 2-6 hr of incubation they were fixed with ice cold 70 % ethanol for 15 min. Cell plasma membrane was visualized by staining with Texas Red C2-maleimide (Texas Red, 30 ng/ml in PBS, Invitrogen, Carlsbad, CA, USA) as described before[23]. Cell nuclei were counterstained with Hoechst 33258 (1 µg/ml in PBS, Sigma). Ten random pictures were taken by IX-70 microscope, equipped with a DP-71 digital camera (Olympus, Japan). Cell attachment area, perimeter and Feret's diameter of 30 cells for each group were measured by Image J software (NIH, USA).

B. Actin cytoskeleton organization and focal adhesion formation

For immunostaining of cytoskeleton and focal adhesions the cells were seeded at the initial seeding density of 5.0×10^3 cells/cm^2 and after 2-6 hr of incubation they were fixed with 3.7 % (v/v) neutral buffered formalin. The cells were then permeabilized with 0.25 % (v/v) Triton X-100 solution and incubated with 1% (w/v) BSA solution to block unspecific antibody binding. To visualize the focal adhesions the cells were then incubated overnight at 4°C with monoclonal anti-vinculin (dilution 1:60, Santa Cruz Biotechnology, Santa Cruz, CA, USA). After rinsing with PBS, the samples were incubated for 1 hr at room temperature in a solution of secondary antibody, goat anti-mouse IgG conjugated with Texas Red (dilution 1:100, Santa Cruz) mixed with Alexa (488)-conjugated phalloidin (5 U/ml, Invitrogen) to visualize actin cytoskeleton. After washing with PBS

the nucleus was counterstained with Hoechst 33528 as mentioned above and the samples were mounted in aqueous mounting medium (Dako Faramounts, Dako North America Inc., CA, USA) and evaluated under a fluorescence microscope.

C. Western blot analysis of vinculin

For western blot analysis of vinculin expression, mesenchymal stem cells were seeded at disks of diameter 20 mm in 12-well plate at initial density of 1.5×10^5 cells/well and incubated for 12 hr in a CO_2 incubator. At the given times the disks were rinsed twice with ice cold PBS and the cells were lysed with ice cold RIPA buffer. The cell lysate was collected and centrifuged at 14 000 × g for 15 min at 4°C. Protein concentration in the solution was determined by DC Bio-Rad assay according to the manufacturer's protocol (BioRad Laboratories Inc., Hercules, CA, USA). The samples were mixed with SDS-PAGE loading buffer supplemented with 5 % β-mercaptoethanol (total protein amount 8 µg), denatured by heat (95°C, 5 min) and then loaded to 11 % polyacrylamide gels. The proteins were separated by electrophoresis and then transferred to PVDF membranes. After blocking the membranes in 5 % skim milk (Difco Laboratories, BD, France) they were incubated for 1 hr with mouse monoclonal anti-vinculin (dilution 1:5000) or mouse monoclonal GAPDH antibody (dilution 1:8000, Chemicon International, Temecula, CA, USA) for control of protein loading and standardization of results. Finally, the membranes were incubated with secondary antibody (goat anti-mouse IgG conjugated with horse radish peroxidase, dilution 1:2000, Santa Cruz). Chemiluminescent detection of membranes was performed using the West-Q Chemiluminescent Substrate kit (GenDEPOT, Barker, TX, USA)

and high-performance chemiluminescence film (Amersham Hyperfilm ECL, GE Healthcare Limited, UK). Densitometry of bands was performed using the Image J software.

8. Serum free culture

Cell adhesion to disks in serum free media was determined to confirm the effect of the proteins adsorbed to titanium. The disks were coated with fibronectin (20 μg/ml in PBS) 1 hr at 37°C and then washed 2 times in PBS. To prevent unspecific binding, the disks were then blocked with 5% (w/v) BSA (in PBS, 30 min at 37°C) and washed again. Disks coated with 5% BSA (in PBS, 1 hr at 37°C) were used as negative controls. Cell adhesion to non-coated disks was also observed.

The MSC cells were pretreated with cyclohexamidine 4 hr before cell seeding (20 μg/ml in serum free media, Sigma) and the attachment time was shortened to one hour in order to prevent the effect of matrix proteins secreted by the cells, which would comprise the analysis of cell adhesion to the pre-coated proteins[24]. After detaching the cells by trypsinization and centrifugation, they were resuspended in serum free media and seeded to the prepared disks at density of $2.5 \times 10^4/cm^2$. After the incubation, cell adhesion was determined by MTT assay as described before.

9. Cell proliferation assay

For proliferation assay the cells were plated at an initial density of 1.0×10^4 cells/cm^2 and incubated for 1, 3, or 5 days in a CO_2 incubator. At the given times cell number was determined by MTT assay as described before.

10. Osteoblastic differentiation – ALP activity

Osteoblastic differentiation in DPC cells was induced by supplementing the cell culture media with sodium ascorbate (50 μg/ml), a source of inorganic phosphate, β-glycerol phosphate (10 mM), and dexamethasome (10^{-8} M) one day after the seeding.

To determine alkaline phosphatase activity, the cells were seeded at the initial density 7.0×10^3 cells/cm^2. Osteogenic media was supplemented 24 hr after seeding and exchanged every 3 days. At given times of culture (5-12 days after seeding) the cells were rinsed with PBS and lysed with 1% Triton X-100 in Tris/$NaHCO_3$ buffer (12.5 mmol/l each, pH 6.8). ALP activity in the cell lysate was determined by a colorimetric assay using phosphatase substrate (pNPP, Sigma). Cell lysates were mixed with 10 mM pNPP solution in glycine buffer as described before and incubated at 37°C. After 30 min the optical density at 405 nm was read spectrophotometrically. At the same time protein concentration in the cell lysates was determined by bicinchoninic acid assay (BCA, Pierce) according to the protocol for 96-well plate as provided by the manufacturer.

11. Statistical analysis

All results are expressed as mean ± standard error of mean (SEM) and analyzed by Student t-test. Statistical significance was considered at $p<0.05$.

III. RESULTS

1. Surface characteristics of titanium samples

A. Surface chemistry

Two major changes in surface characteristics after He-APGD treatment could be observed with X-ray photoelectron spectroscopy which are summarized in Figure 2D.

The first is a decrease in relative atomic concentration of carbon (Figure 2A). Narrow-scan spectra of C 1s around 285 ~ 289 eV show a rapid drop of peaks corresponding to C-C, C-O and C=O already after 3 s of plasma treatment and then continual, although small decrease with the increasing treatment time.

The second narrow-scan spectra of O 1s (Figure 2B) shows relative dropping of oxygen neighbor shoulder broadly around 532.3 eV in 3 s He-APGD treated surface, which then recovers around 531.9 eV in titanium treated for 1 min or longer.

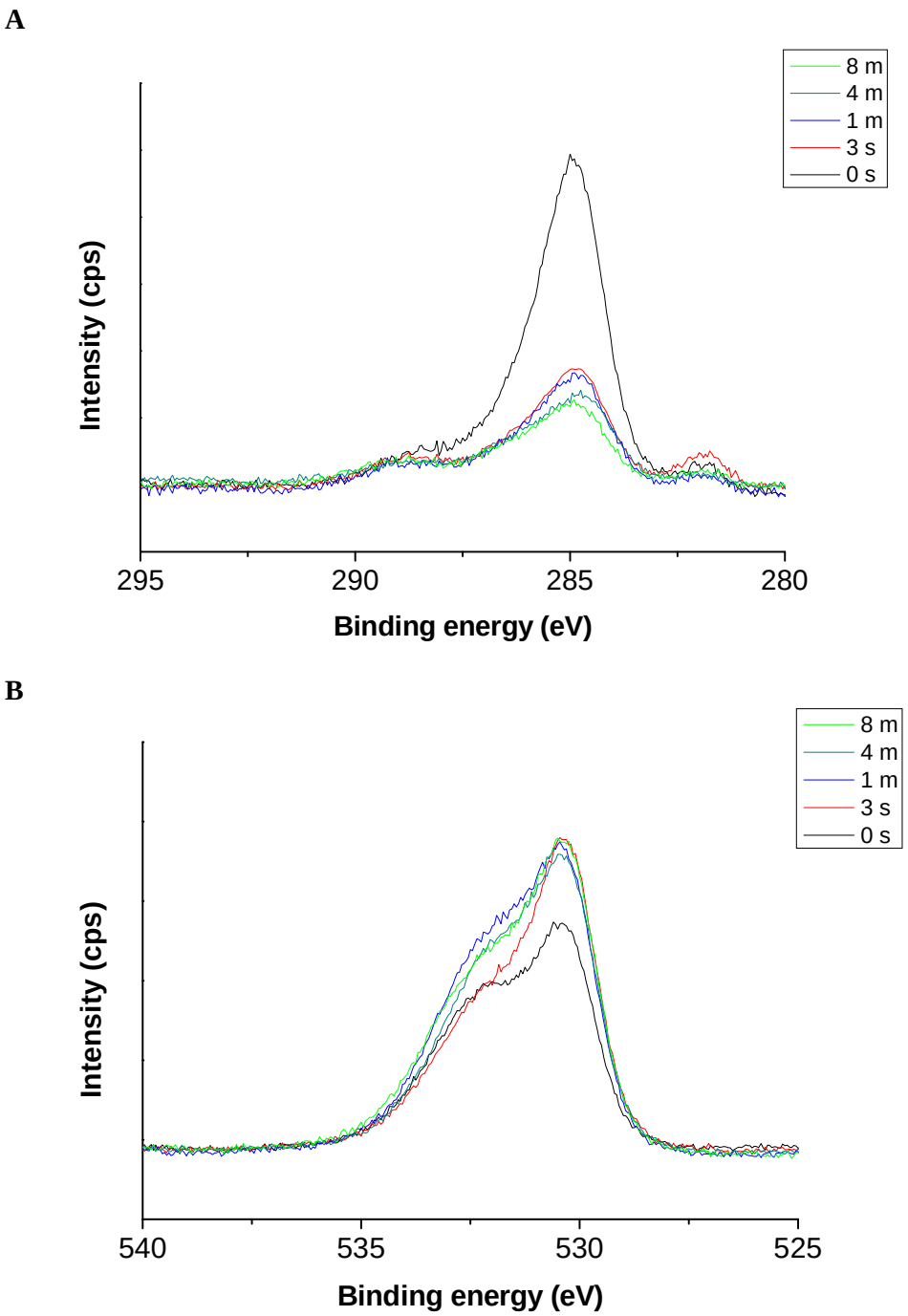

Figure 2. XPS analysis of He-APGD treated titanium. XPS narrow-scan spectra of (A) C 1s and (B) O 1s.

C

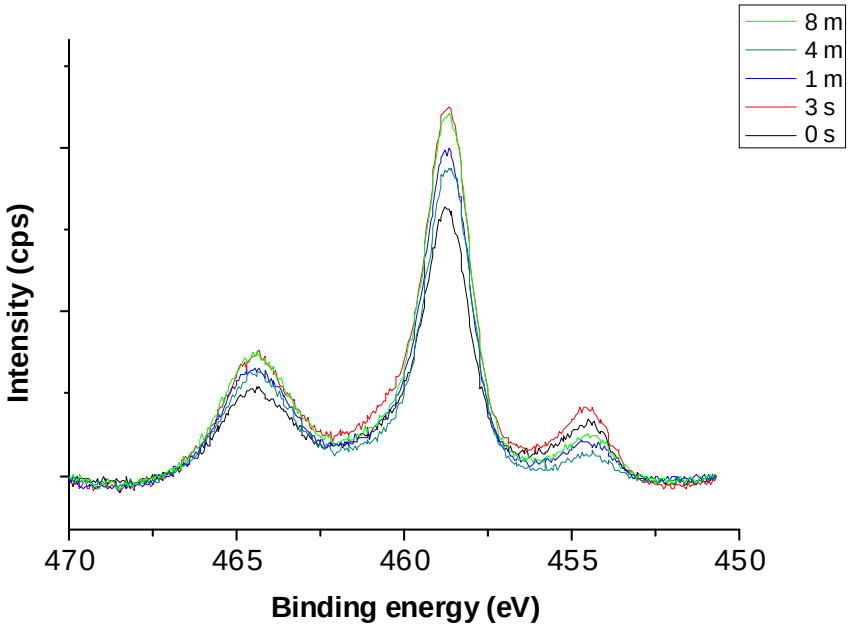

D

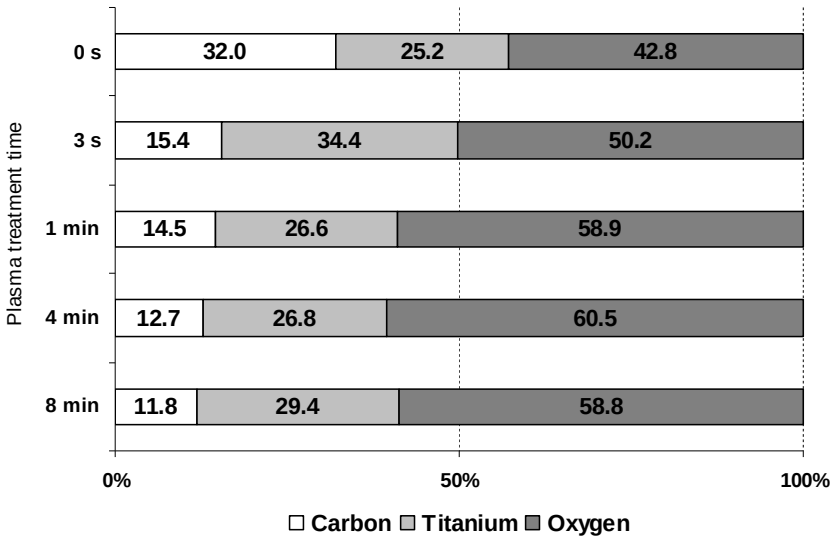

Figure 2. XPS analysis of He-APGD treated titanium. (C) XPS narrow-scan spectra of Ti 2p. (D) Surface composition of He-APGD-treated titanium.

B. Wettability

He-APGD treatment of titanium rendered the surface high hydrophilicity (Figure 3A). The water contact angle fell from 57 degrees on the untreated sample to about 15 degrees already after 3 s of treatment. The spreading of the water drop increased with the increasing plasma treatment time. After 8 min treatment the surface became superhydrophilic and it was not possible to measure the water contact angle as the drop spread completely over the sample.

Recovery of these hydrophilic characteristics was observed by water contact over 4 weeks (Figure 3B). In both 3 s and 8 min treated samples the wettability restored only up to 30 degrees in one month.

A

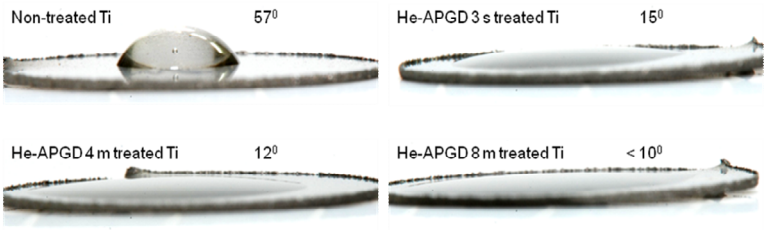

B

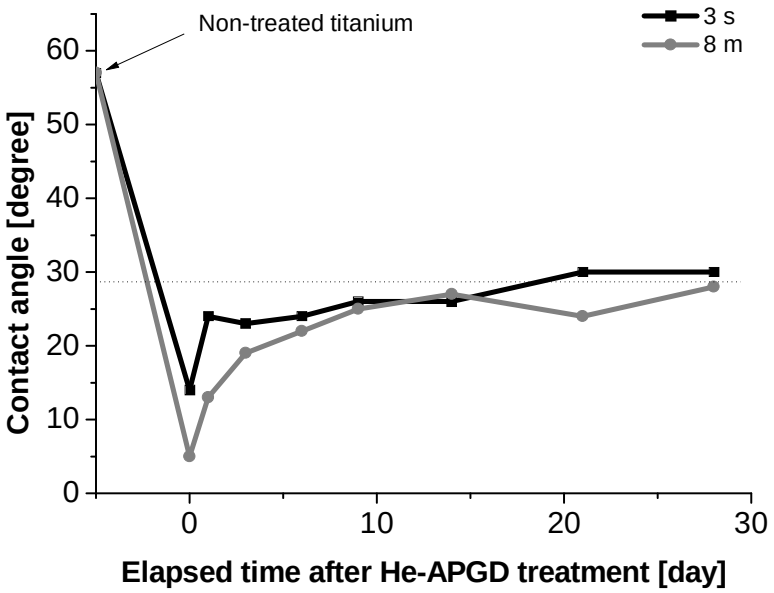

Figure 3. Changes in hydrophilicity of titanium after He-APGD treatment.

(A) Photographs of distilled water drop on the non-treated and He-APGD treated titanium surfaces. (B) Restoration of hydrophobic characteristics of the titanium surfaces over time.

C. Surface morphology

SEM micrographs (Figure 4) show relatively rough surface of titanium created by the manufacturing process, however there are no visible changes after the plasma treatment.

AFM analysis showed slight changes in roughness and surface topology of titanium samples after the He-APGD treatment on nano-scale level. Root mean square roughness (Rrms) showed more than 5-fold increase from 3.06 nm of the non-treated titanium to 16.29 nm in 3 s treated sample (Table 1). With the increasing treatment time the titanium roughness slightly decreased. Similar pattern was observed also in average roughness (Ra).

Three dimensional topology of titanium surface (Figure 5) changed from relatively smooth with homogeneously sputtered irregular particles before the plasma treatment (A) to a structured with significant surface corrugations after 3 s modification (B). However, with the increasing plasma treatment time, the size and sharpness of the corrugations and ridges seemed to decrease and the surface became smoother (C and D).

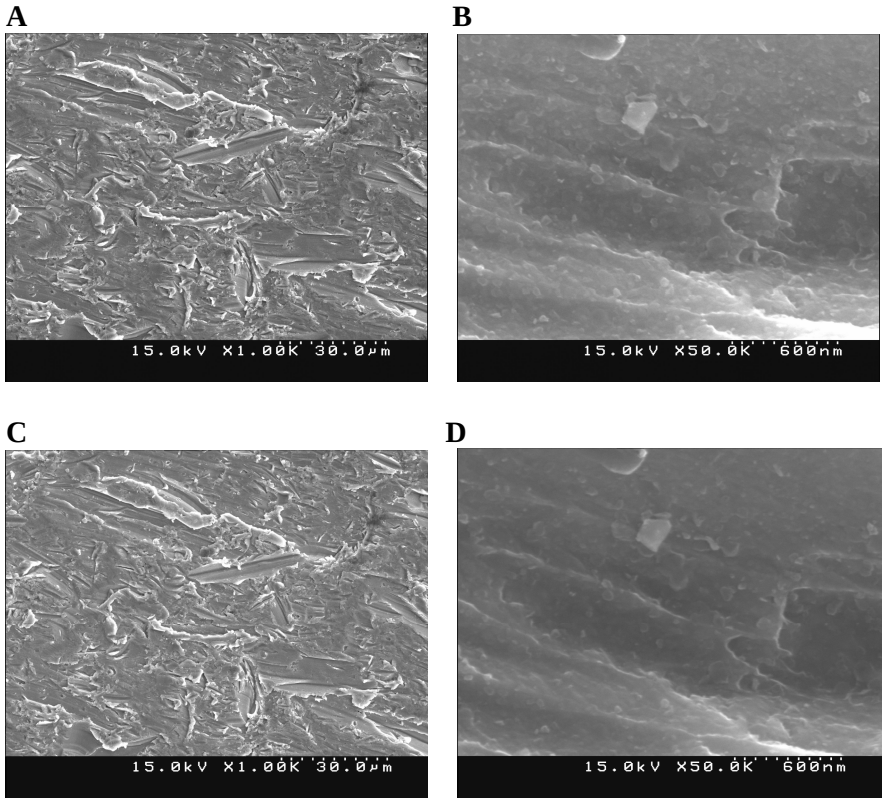

Figure 4. SEM images of titanium disk surface before (A, B) and after 4 min of He-APGD treatment (C, D). Scale bar=30 µm in A, C or 600 nm in B, D.

Treatment time	0 s	3 s	4 min	8 min
Ra [nm]	1.88	12.76	10.54	8.39
Rrms [nm]	3.06	16.29	13.37	10.84

Table 1. Surface roughness of titanium samples before and after He-APGD treatment. Rrms and Ra were determined by AFM analysis, scanning range was 0.5 µm × 0.5 µm.

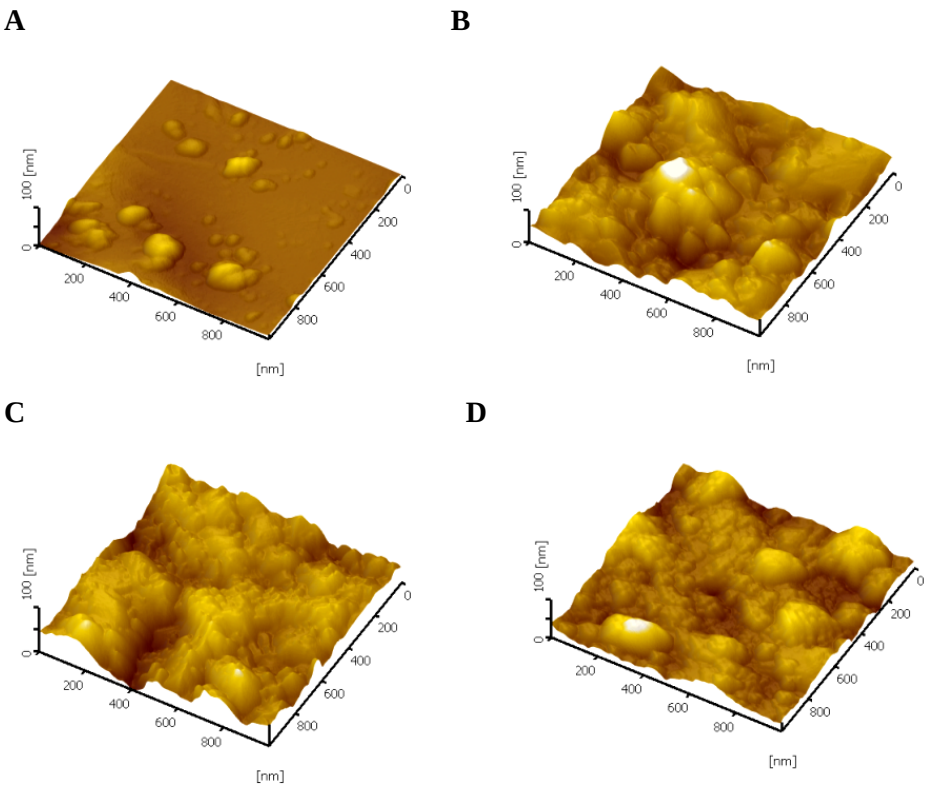

Figure 5. AFM images of titanium disk surface before (A) and after 3 s, 4 min, 8 min of He-APGD treatment (B, C, and D respectively). Scanning range was 1 µm × 1 µm, *z*-axis 100 nm.

2. Protein adsorption

Three different model protein solutions were used to observe protein adsorption after 1 hr incubation with the titanium disks. The micro BCA assay showed no significant difference ($p<0.05$) between the non-treated and He-APGD treated titanium disks in case of fetal bovine serum and bovine serum albumin. However, the plasma treated samples showed higher adsorption of fibronectin than control (Figure 6). The amount of adsorbed fibronectin increased gradually with the treatment time, up to a significant ($p<0.05$) 2-fold increase at 8 min. Relative increase about 10 - 16 % in fibronectin adsorption on the plasma treated samples was confirmed also by anti-fibronectin antibody detection by a modified ELISA method (Figure 7).

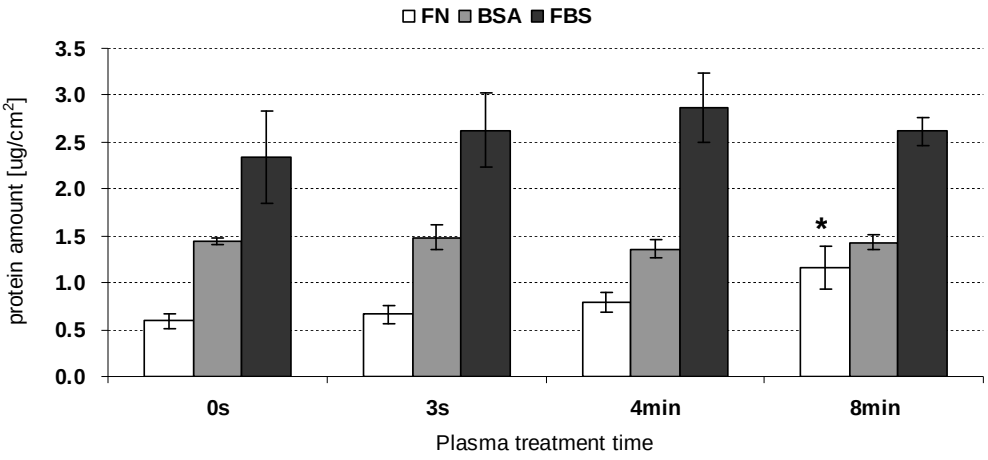

Figure 6. Fibronectin (FN), bovine serum albumin (BSA) and fetal bovine serum (FBS) adsorption to He-APGD treated titanium disks after 1hr incubation at 37°C as determined by microBCA assay. The results are shown as a mean ± standard error of mean (SEM) (n=4). The data were analyzed by Student t-test (* $p<0.05$ in comparison with the control, 0 s).

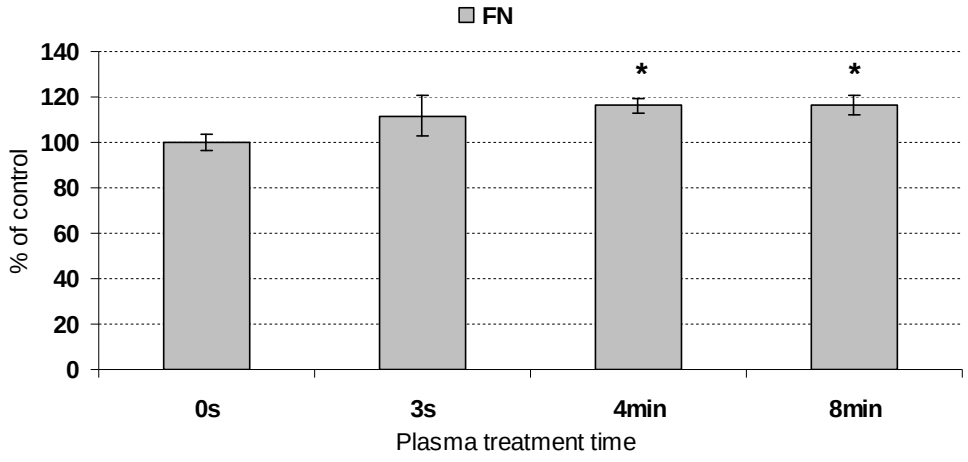

Figure 7. Fibronectin (FN) adsorption to He-APGD treated titanium disks after 1hr incubation at 37°C as determined by ELISA method. The results are shown as mean ± standard error of mean (SEM) (n=4). The data were analyzed by Student t-test (* $p<0.05$ in comparison with the control, 0 s).

3. Cell initial adhesion

Figure 8 shows the effect of He-APGD treatment on the number of attaching cells to the titanium disks shortly after seeding (2 hr in MC3T3-E1 and MSC or 6 hr in DPC) as determined by MTT assay. Mouse pre-osteoblasts, MC3T3-E1 cells, 2 hours after seeding seemed to adhere better to samples that were treated with He-APGD. The number of attached cells increased from 20 to 35%, this difference was however, significant only at 4 min treated samples ($p<0.05$). Slightly higher enhancement of attachment (from 25 to 37%) was observed also in primary culture of dental pulp cells 6 hrs after seeding (DPC cells require longer time for attachment). Most significant ($p<0.01$) improvement of cell adhesion provided the plasma treatment in case of human mesenchymal stem cells, where a two-fold increase in cell attachment was observed on all He-APGD treated samples. In all cell types plasma treatment enhanced initial cell adhesion, but there seemed to be no dependence of the number of attached on the treatment time.

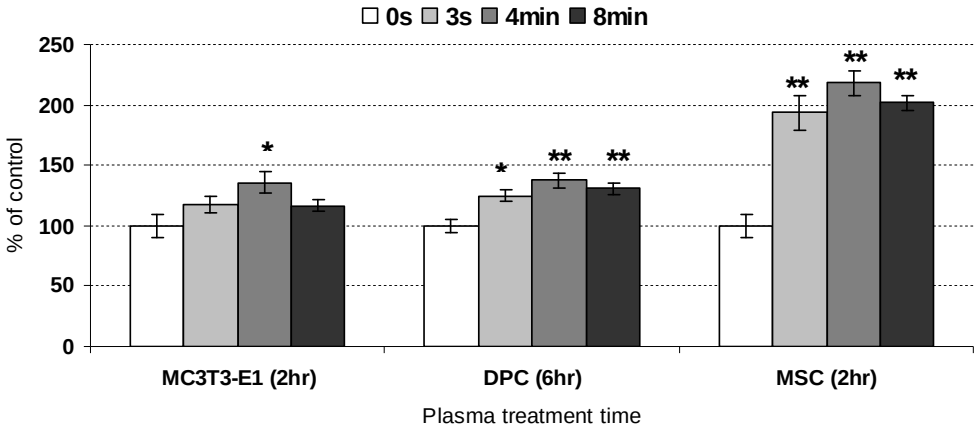

Figure 8. Effect of He-APGD treatment on the initial adhesion of cells. The number of attached cells is expressed as % of attachment on the non-treated disks (0s) as evaluated by MTT assay. The results are shown as mean ± standard error of mean (n=4). The data were analyzed by Student t-test (* $p<0.05$, ** $p<0.01$ in comparison with the control, 0 s).

4. Cell morphology

A. Cell adhesion area

Fluorescence pictures of cells on the titanium disks after visualizing the plasma membrane by Texas Red maleimide staining have shown that already 2 hr after seeding (or 6 hr for DPC), not only the number of attached cell is higher on plasma treated samples, but they were also clearly larger. Cells adhering to non-treated disks were smaller and round-shaped, while cells on He-APGD treated disks had larger attachment area, well-spread elongated morphology with formed lamellipodia-like projections (Figure 9, 10 and 11). Their size also seemed to increase proportionally with the increasing plasma treatment time, especially in primary cultures of DPC and MSC.

These observations were also confirmed by morphometric measurements in Image J software. Cells growing on plasma treated samples had significantly ($p<0.05$) higher Feret's diameter (the longest axis of cell), perimeter and attachment area (Figure 12). Moreover, in all cell types these three parameters increased proportionally with the increasing plasma treatment time.

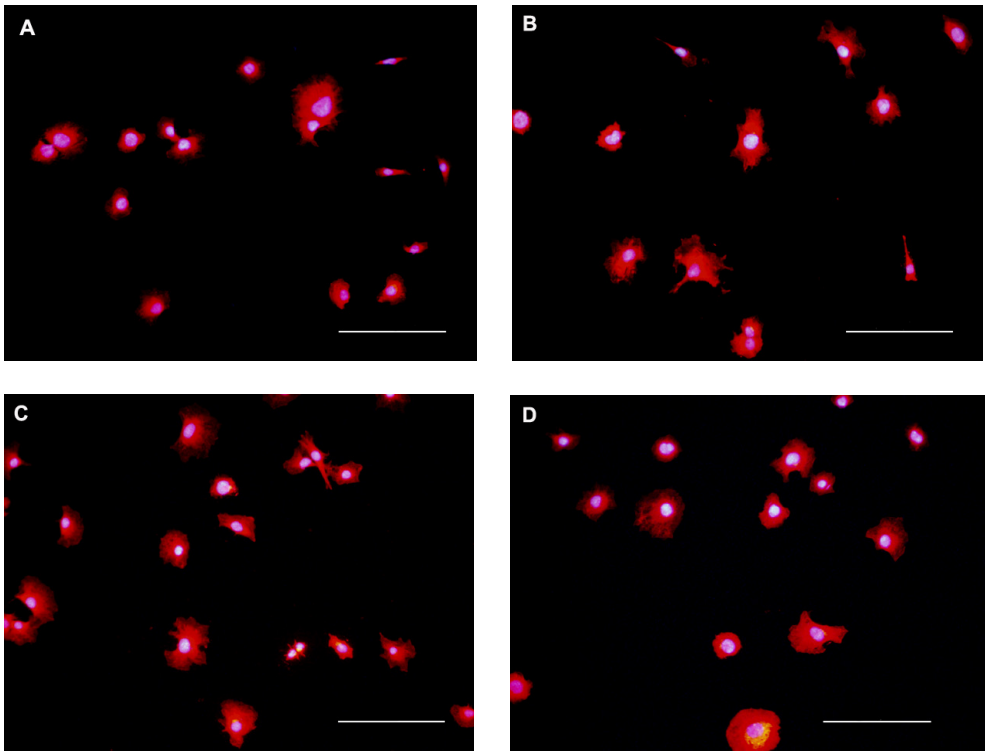

Figure 9. Morphology of MC3T3-E1 cells on He-APGD treated titanium.

Initial spreading of mouse pre-osteoblasts on non-treated (A) and 3 s, 4 min and 8 min (B, C and D respectively) plasma treated titanium, 2 hr after seeding. Plasma membrane was stained with Texas Red maleimide C2 (red) and nucleus with Hoechst 33258 (blue). Fluorescence microscopic images were taken with Olympus inverted microscope (IX-70, obj. 20 ×) equipped with DP71 camera. Scale bar=200 μm.

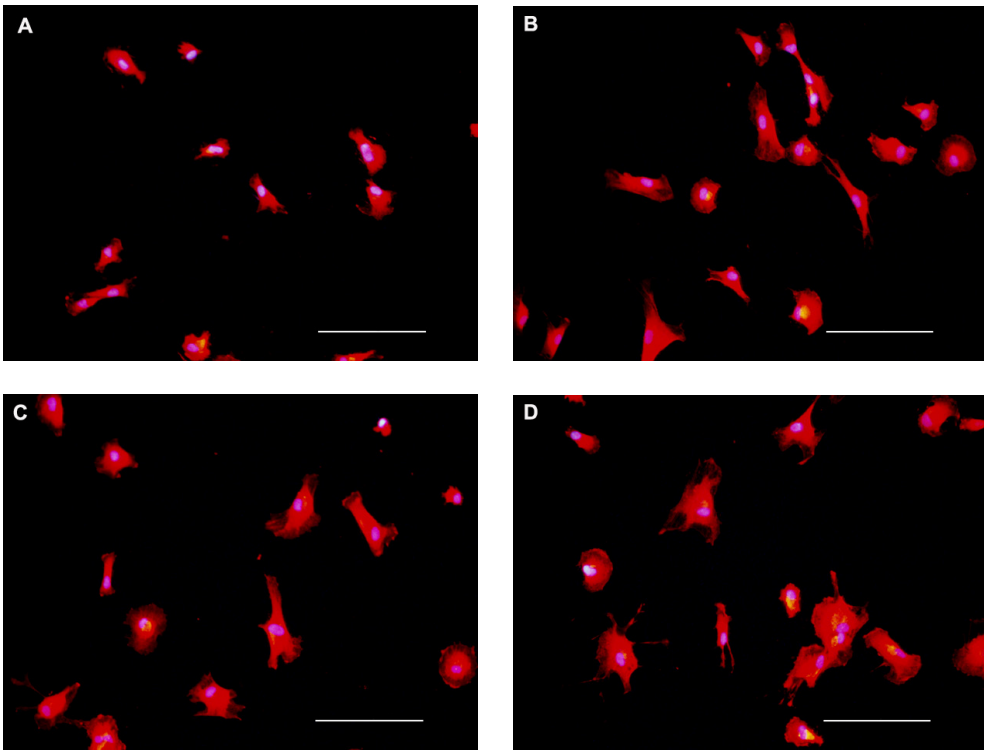

Figure 10. Morphology of dental pulp cells on He-APGD treated titanium.

Initial spreading of DPCs on non-treated (A) and 3 s, 4 min and 8 min (B, C and D respectively) plasma treated titanium, 6 hr after seeding. Plasma membrane was stained with Texas Red maleimide C2 (red) and nucleus with Hoechst 33258 (blue). Fluorescence microscopic images were taken with Olympus inverted microscope (IX-70, obj. 20 ×) equipped with DP71 camera. Scale bar=200 μm.

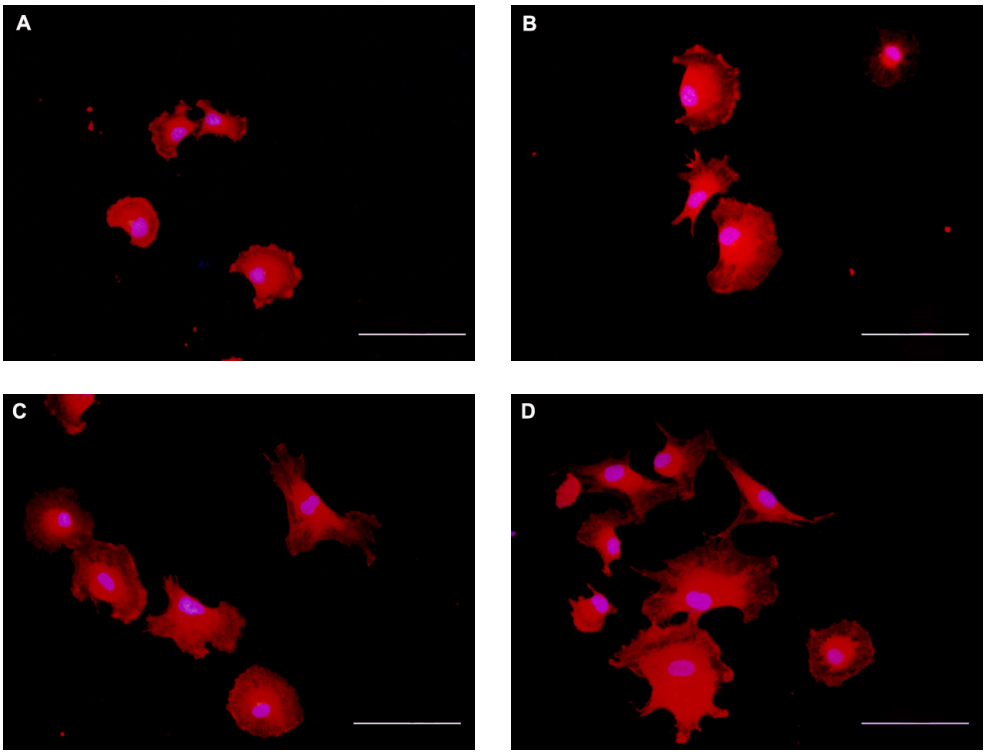

Figure 10. Morphology of mesenchymal stem cells on He-APGD treated titanium. Initial spreading of MSCs on non-treated (A) and 3 s, 4 min and 8 min (B, C and D respectively) plasma treated titanium, 2 hr after seeding. Plasma membrane was stained with Texas Red maleimide C2 (red) and nucleus with Hoechst 33258 (blue). Fluorescence microscopic images were taken with Olympus inverted microscope (IX-70, obj. 20 ×) equipped with DP71 camera. Scale bar=125 μm.

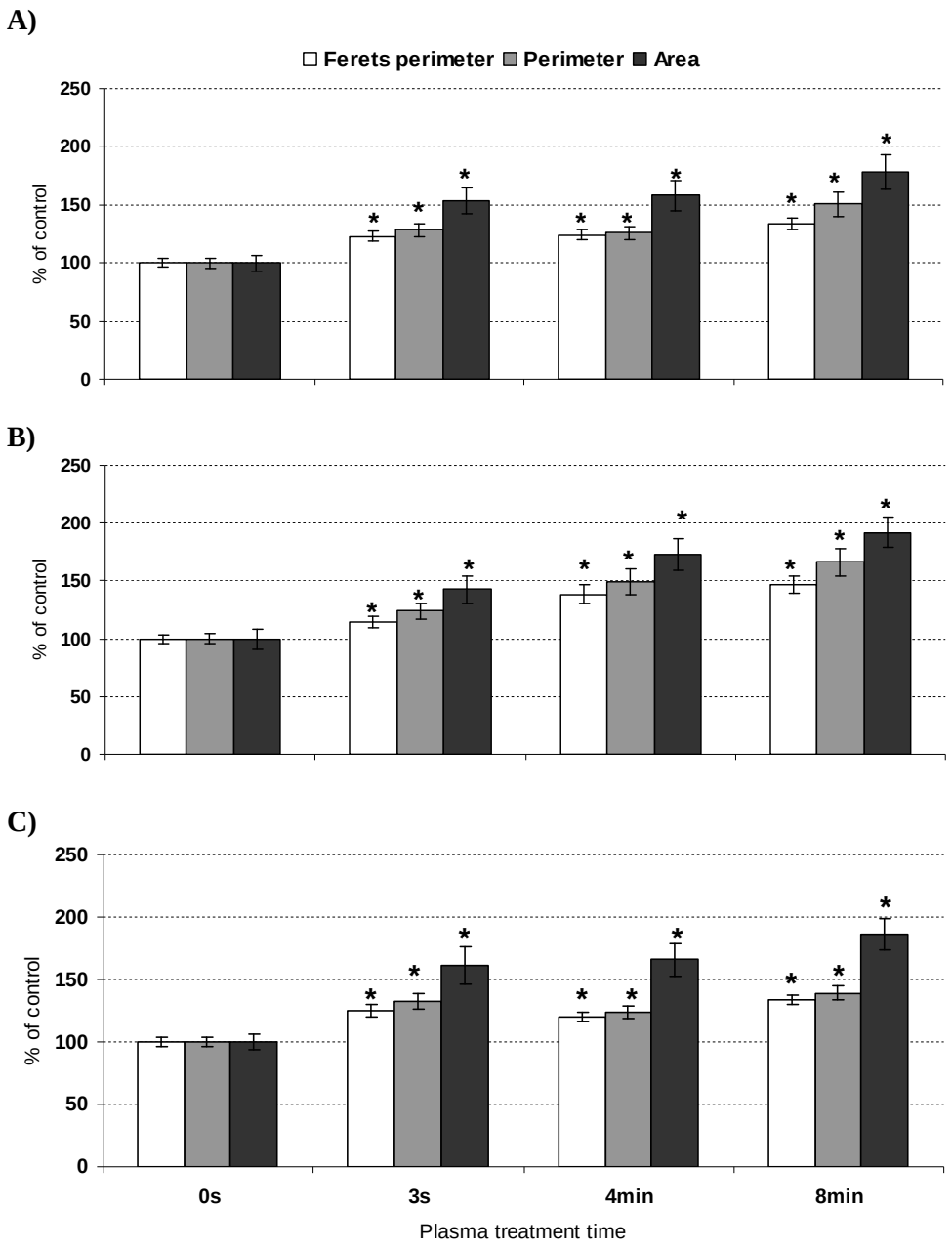

Figure 11. Cell morphometric measurements. Attachment area, perimeter and Feret's diameter of A) MC3T3-E1 B) MSC and C) DPC cells were measured from micrographs by Image J software. The results are shown as mean ± standard error of mean (n=30). The data were analyzed by Student t-test (* $p<0.05$).

B. Focal adhesion formation and actin cytoskeleton organization

After 3 hr (MC3T3-E1 and MSC) or 6 hr (DPC) of incubation, actin cytoskeleton organization and focal adhesion formation was observed by Alexa 488 conjugated-phalloidin and anti-vinculin immunostaining respectively. As shown in Figure 13 (A-C), for all cell types, the shape and size of cell body was clearly different on He-APGD treated samples. Cells attached to non-treated titanium surface were smaller, in DPC and MSC still round-shaped and their cytoskeleton was not yet well-developed. Actin was diffuse in cell cytoplasm and only short, thin fibers could be observed especially in the cell periphery. Similarly, vinculin staining showed that even though all cells expressed vinculin, it was diffused evenly in the cell cytoplasm, and only small, not very distinct focal adhesions could be found on the cell periphery. In contrast, cell attached to the plasma treated samples were larger, had elongated shape and formed lamellipodia-like projections that were enforced with clear stress fibers. Vinculin-positive focal adhesions were observed especially at the ends of these actin filaments, in the elongated projections.

Enhanced vinculin expression on plasma treated titanium disks was also confirmed by western blot analysis (Figure 14).

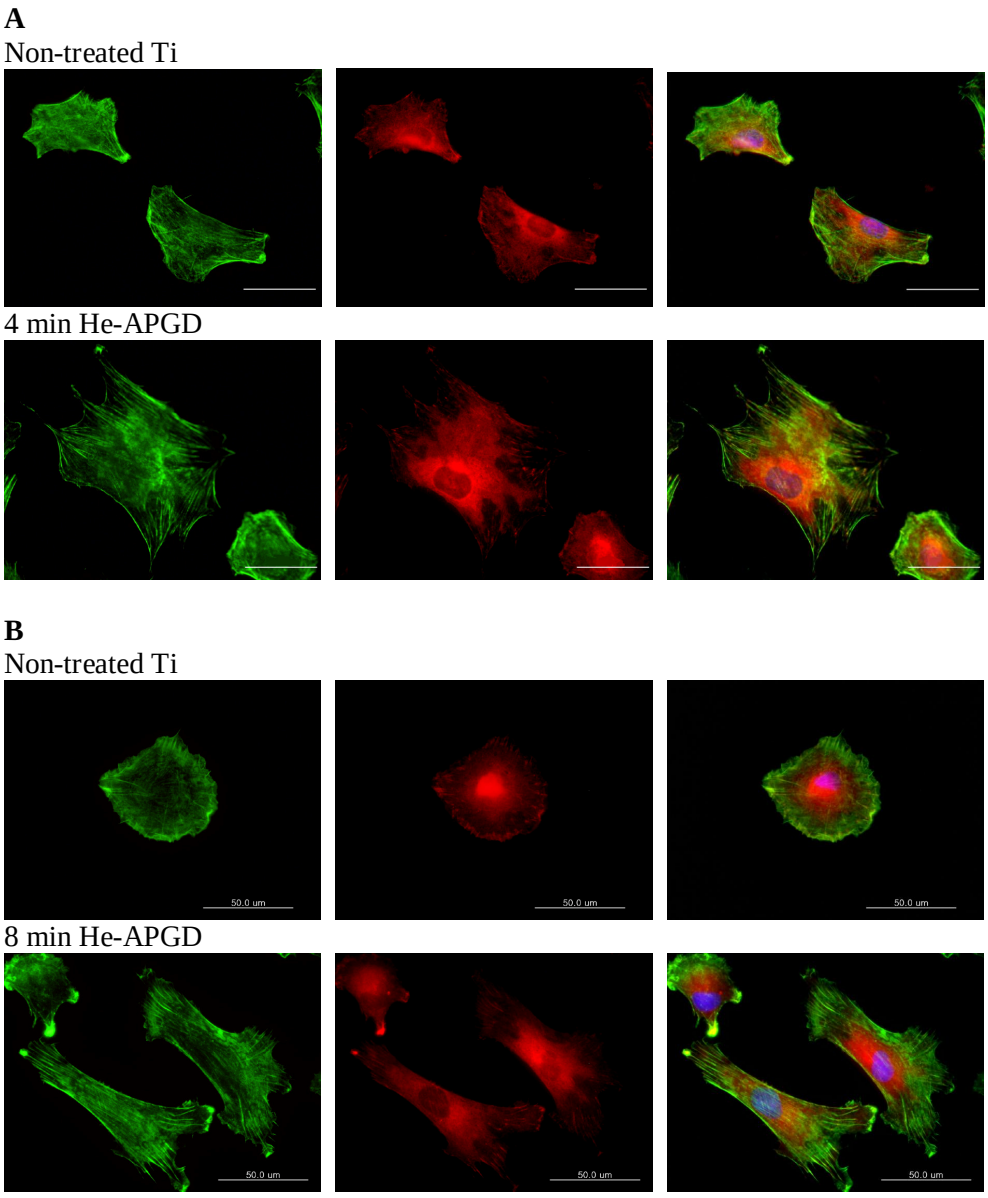

Figure 13. Actin cytoskeleton arrangement and focal adhesion formation.

Representative fluorescence microscopic images of (A) MC3T3-E1 and (B) MSC cells stained with Alexa 488-conjugated phalloidin against actin filaments (green) anti-vinculin (red) and Hoechst 33258 for nucleus (blue). Scale bar=50 μm.

C

Non-treated Ti

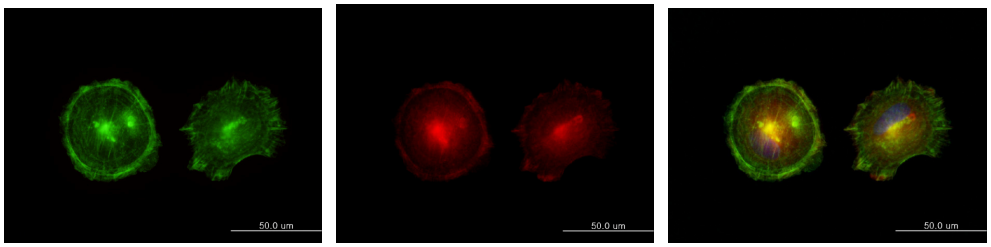

8 min He-APGD

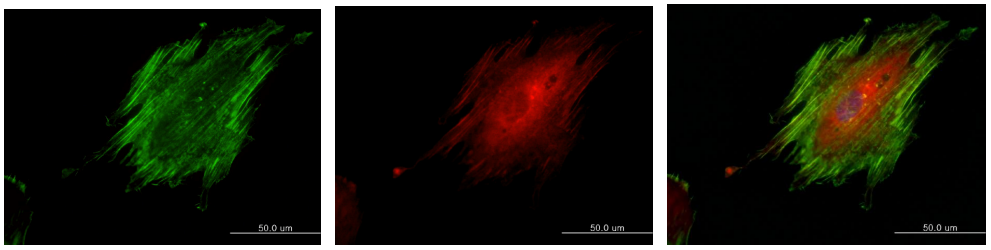

Figure 13. Actin cytoskeleton arrangement and focal adhesion formation.

Representative fluorescence microscopic images of (C) DPC cells stained with Alexa 488-conjugated phalloidin against actin filaments (green), anti-vinculin (red) and Hoechst 33258 for nucleus (blue). Scale bar=50 μm.

A

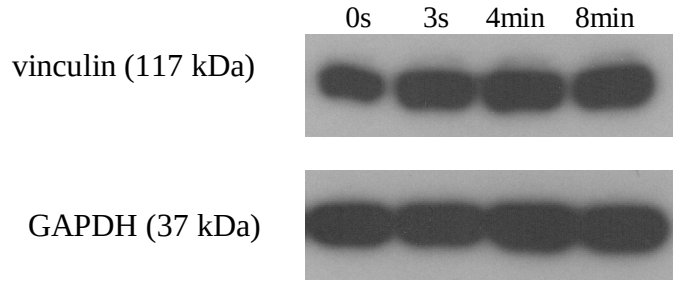

B

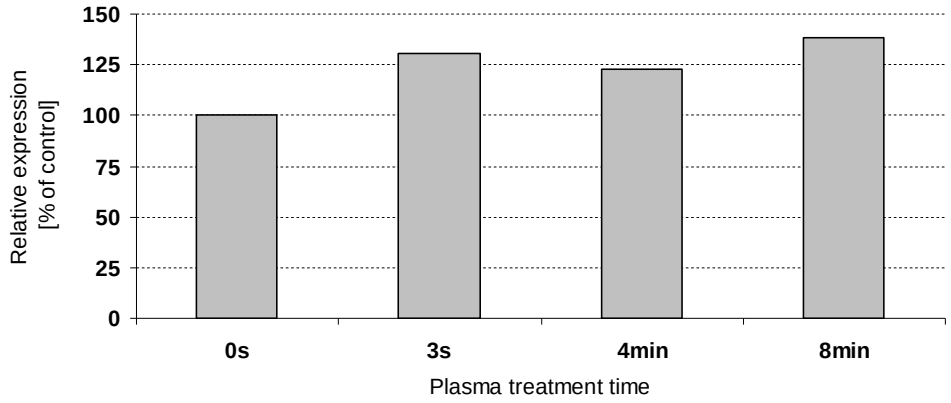

Figure 14. Western blot analysis of vinculin expression in MSC cells on plasma treated Ti disks. (A) Representative western blot images for vinculin and GAPDH (control) from MSC lysates obtained 12 hr after seeding. (B) Relative vinculin expression as determined by densitometry by Image J software. Data are expressed as % of vinculin expression on the control (0s) sample.

5. Serum free culture

In order to examine the mechanism by which cells attach to plasma treated titanium, an attachment assay to fibronectin pre-coated or non-coated samples in serum free culture media was performed. Attachment of MSC cells to He-APGD treated disks coated with fibronectin just one hour after seeding was significantly ($p<0.05$) higher than to non-treated disks coated with fibronectin under the same conditions (Figure 15A). There was a 2-fold increase in cell attachment to 4 and 8 min treated samples. Coating of the disks with albumin prevented cell adhesion comparably on all samples, allowing only around 15 % adhesion of the control sample.

Interestingly, a similar pattern was observed in MSC cell adhesion to non-coated titanium disks, also in serum free conditions. The absolute number of attached cells, as well as the relative enhancement by He-APGD was almost the same as on fibronectin coated titanium disks (Figure 15B).

A)

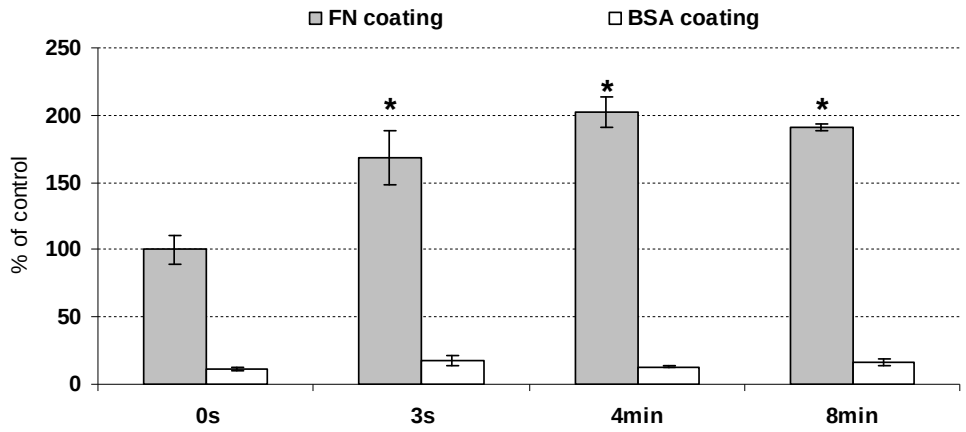

B)

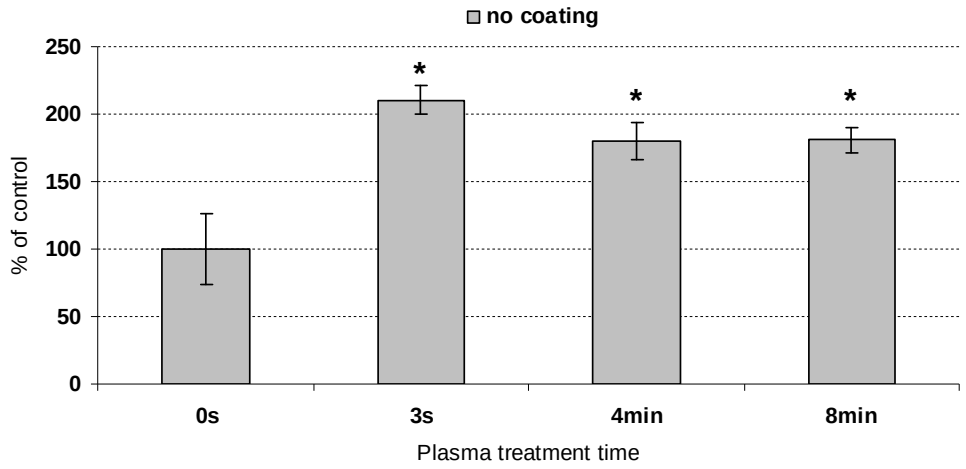

Figure 15. Adhesion of MSC cells to He-APGD treated titanium in serum-free culture. The cells adhesion within 1 hr to (A) fibronectin (20 μg/ml) and BSA (5%) pre-coated; or to (B) non-coated He-APGD treated titanium disks was determined by MTT assay. The number of attached cells is expressed as % of attachment on the non-treated disks (0s). The results are shown as mean ± SEM (n=3,* $p<0.05$ in comparison with the control, 0 s by Student t-test).

6. Cell proliferation

As initial cell adhesion has a great effect on the following cell growth, cell proliferation on He-APGD treated titanium disks was observed up to day 5 after seeding, when the cells reached confluency. In all three tested cell types, the plasma treatment of the sample stimulated their growth rates in a dose-dependent manner (Figure 16). Cell density as determined by MTT assay was higher already 24 hr after seeding on all plasma treated disks. This enhancement was statistically significant ($p<0.05$) from 4 min of treatment. This trend persisted also during the following days of culture (day 3 and 5), and on day 5 the number of cells on 8 min treated samples was from 40 % (MC3T3-E1, DPC) to 120% (MSC) higher than on the non-treated control.

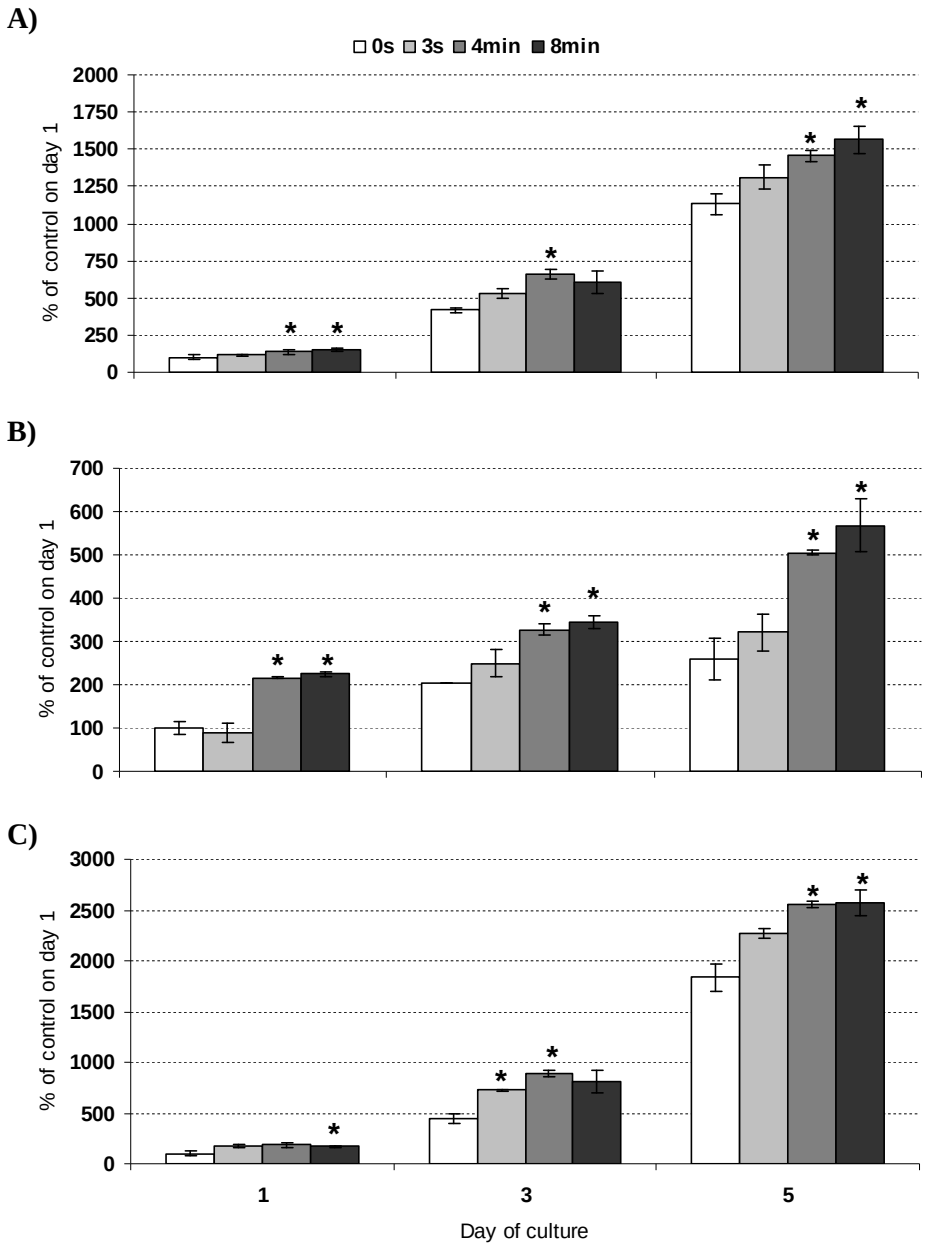

Figure 16. Effect of He-APGD treatment on cell proliferation. Proliferation in (A) MC3T3-E1, (B) MSC and (C) DPC was evaluated by MTT assay. Cell number is expressed as % of control (0s, day 1). The results are shown as mean ± SEM (n=3, * $p<0.05$ in comparison with 0 s by Student t-test)

7. Osteoblastic differentiation - ALP activity

Alkaline phosphatase activity was measured over 12 days of culture as an early marker of osteoblast differentiation in dental pulp cells stimulated by osteogenic media (Figure 17). Already from day 5 there was a significant ($p<0.05$) increase in ALP activity in cells that were treated with osteogenic media in comparison with the control sample grown in a regular culture media. In He-APGD treated samples the activity continued to rise steadily up to day 10 when it reached its peak. After that, it already showed a declining trend. The ALP activity of cells in positive control (cells on TCPS in osteogenic media) and on non-treated titanium samples continued to increase even after day 10 and did not reach their peak before the end of this assay (day 12). Therefore at day 12 their ALP value seemed higher than on the treated samples, even though this difference was statistically significant ($p=0.013$) only in comparison with the 8 min sample.

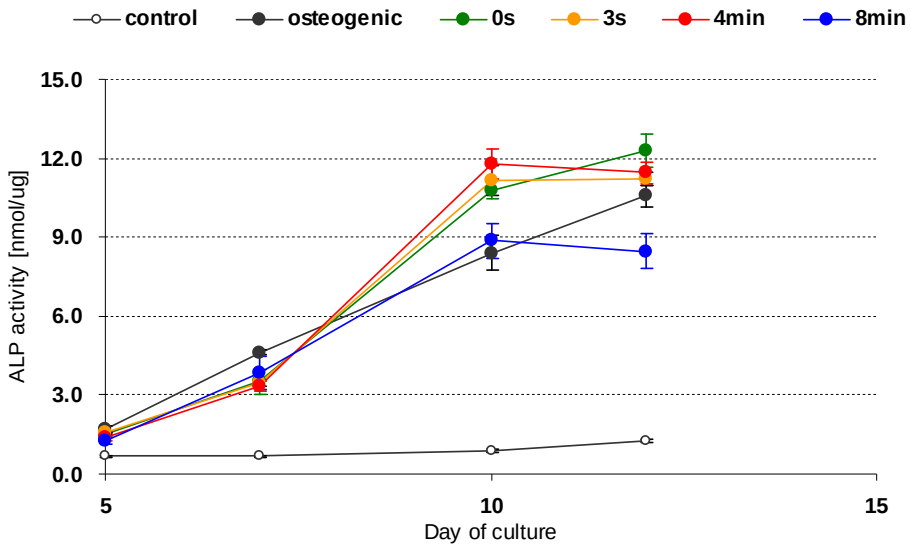

Figure 17. Alkaline phosphatase activity in dental pulp cells on He-APGD treated titanium. The data are shown as mean ± standard error of mean (n=3).

IV. DISCUSSION

In order to evaluate the effect of helium atmospheric pressure glow discharge treatment on titanium surface both surface chemistry and morphology were examined.

Changes in the surface chemistry of He-APGD were examined by XPS. The analysis has revealed two major changes in the surface properties corresponding to two consecutive events. The first was elimination of carbohydrate contaminants as confirmed by a rapid decrease in relative atomic concentration of carbon already after 3 s of plasma treatment. Decrease in carbon peak was also accompanied by a drop in peaks of carbon-oxygen bondings present in hydrocarbon molecules (O-C, O=C) in narrow spectra of O 1s. Surfaces tend to bind molecules or atoms from surroundings which form a layer of contaminants. Typically these impurities are hydrocarbons which are present in the ambient air[5, 25]. This layer of hydrocarbon contamination passivates the surface, hinders further bond formation, resulting in a lower surface energy and water repelling, hydrophobic character[26], which may have a great effect on biological responses. Hydrocarbon contaminant elimination was suggested to be also the main underlying reason in enhanced mesenchymal stem cell response and faster tissue integration of UV-treated titanium[27, 28].

The second process was grafting of hydroxyl groups, as shown by the recovery of the oxygen neighboring shoulder after 1 to 8 min of treatment. The increase in hydroxyl group shoulder was not accompanied with a concomitant recovery

in carbon-oxygen bonds, therefore it can be suggested that Ti-OH groups have been formed as a result of the treatment.

Elimination of surface hydrocarbon contaminants and engraftment of hydroxyl groups increase the hydrophilicity of metal surfaces. Wettability measurements in He-APGD treatment of titanium have confirmed rapid fall in water contact angle already after 3 s treatment and after 8 min of modification the surface became superhydrophilic (WCA<5°). In general, the plasma-treated surfaces tend to lose modified hydrophilicity over time, which may be due to the release of excited energy obtained from plasma. Water contact restoration was observed over a period of one month and the results showed that even after this period the water contact angle has restored only up to 30°. In comparison with other superhydrophilic surfaces, such as UV-treated titanium, He-APGD treated surface exhibited significant resistance to recovery[27].

Increased hydrophilicity and hindered recovery of hydrophobic characteristics of He-APGD treated titanium could be explained not only by hydrocarbon elimination but also by two other processes. First, five-fold titanium found on the surface of native titanium oxide supports water physisorption and dissociative hydroxyl group chemisorption. Furthermore, it was reported that UV irradiation and electron irradiation, which are both present in glow discharge, create surface oxygen vacancies, converting Ti^{4+} state of the six-fold titanium atoms to Ti^{3+} state by breaking oxygen bonding. The increased driving force to stabilize Ti^{3+} sites makes the Ti^{3+} sites preferably bind oxygen derivatives such as atomic oxygen or dissociative hydroxyl group from water molecule[29-32].

Changes in the surface morphology of He-APGD treated titanium surface were examined by SEM and AFM analysis. SEM micrographs have shown that titanium disks have relatively rough surface which is the result of the machining process during titanium plate manufacturing process. Even though, SEM images did not show any visible changes in the gross surface morphology after the plasma treatment, AFM analysis revealed changes in surface roughness and topology on the nanoscale. On the smooth untreated surface numerous irregular particles were visible, which are believed to be impurities and contaminations. The dramatic change in surface topology after the 3 s He-APGD treatment could be therefore ascribed to the cleansing effect of plasma and supports the XPS results of reduced contamination. With the increasing treatment time the surface roughness decreased from 16.29 nm after 3 s to 10.84 nm after 8 min. This could be ascribed to oxidation process and deposition of new titanium oxide on the sample surface. These results are consistent with previous studies, which have reported gradual decrease in surface roughness of titanium[25, 33] or steel[34] after plasma treatment.

Surface morphology both on micro and nanoscale levels influences the following biological responses. While there is still much controversy about the effect of microroughness[35, 36], a considerable attention has been paid in recent years to the nanoscale structure of the material surface. Nanotopography in titanium and other materials has been found to have significant positive effects on osteoblast cell response, including initial cell adhesion and subsequent proliferation, and expression of differentiation markers[37-40]. Plasma treatment not only introduced nanoscale amorphous morphology but also, as suggested by Lin *et al.*[33]

the cleansing effect of plasma treatment provides a larger surface area for protein binding and cell attachment, and could therefore contribute significantly to the increase in bioactivity of plasma treated surfaces.

Interaction of cells with the titanium surface layer of its oxide is mediated by a layer of proteins that adsorbs to the implant surface from plasma or other physiological fluids. The composition of the adsorbed layer varies greatly according to surface properties of the substrate and may differ substantially. This layer mediates integrin-receptor based cell adhesion and proliferation and determines the cellular response to the biomaterial[41, 42].

He-APGD treatment of titanium did not have a significant effect on the amount of adsorbed proteins from the fetal bovine serum or bovine serum albumin solution. However, a gradual increase in the amount of adsorbed fibronectin from a single protein solution with the increasing plasma treatment time was observed. These results are consistent with the observations of Pegueroles *et al*. who found that the amount of adsorbed FN correlates with wettability and surface energy rather than surface roughness[43]. Fibronectin is one of the earliest proteins laid down in extracellular matrix and is required for recruitment of growth factors and assembly of other ECM proteins[44-46]. It is a soluble protein and it is well-established that it has critical role in osteoblast adhesion to biomaterials, their survival and the following differentiation. Fibronectin adsorption in competition with other proteins, especially non-adhesive albumin, that has a 200-fold higher concentration in human plasma, is a crucial step for cell adhesion ability[47]. Therefore it could be

suggested that the selective enhancement of fibronectin adsorption to plasma treated titanium is the major underlying mechanism of increased cellular response.

To confirm this hypothesis MSC attachment to FN pre-coated samples in serum free media was performed. The attachment time was reduced to one hour, because within this short period the amount of ECM proteins secreted by cells themselves is negligible and the cell adhesion depends merely on the pre-adsorbed proteins[24]. The increase in number of attached cells was consistent with the increasing amount of adsorbed FN and moreover the enhancement of cell attachment on He-APGD treated titanium was more significant than in normal cell culture media. More interestingly, increased MSC attachment on plasma treated titanium was observed also on non-coated disks in serum free conditions. Furthermore, the absolute number of attached cells on non-coated disks was comparable with FN-coated disks. Similar pattern was observed also in case of photofunctionalized titanium by UV, and the authors suggested a direct interaction of cells with the sample via an electrostatic mechanism[13]. According to their hypothesis, UV-treated TiO_2 surfaces are electropositively charged because of exited electrons from valence bands to conduction bands, allowing direct attachment of negatively charged cells; as opposed to untreated titanium surfaces that are bioinert and require inorganic and biological bridges (divalent cations and proteins) for cell attachment and adhesion. However, it needs to be noted that this hypothesis of direct cell/titanium interaction is difficult to test, as it is has been previously shown that cell adhesion to substrates in serum-free conditions can occur through secreted FN molecules found on the cell surface[48].

Even though the exact mechanism by which He-APGD enhances cell response is unknown this study shows that the treatment enhances titanium bioactivity. Cell initial attachment, adhesion and spreading belong to the first phase of cell/artificial material interaction, which is crucial not only for cell survival, but also for the following cell growth, proliferation and differentiation. The results have shown that plasma treatment enhanced cell initial attachment in all three types of progenitor cells. Moreover, cell spreading, as shown by morphometric measurements, increased gradually with the increasing plasma treatment time. Spreading of cell is an active process depending on cell adhesion molecules, namely integrin adhesion receptors, which act as the central regulators of cell-biomaterial interaction[49]. After binding their ligands (adhesive peptides with RGD motif such as FN), integrin subunits cluster into supramolecular complexes, focal adhesions. Other proteins such as cytoskeletal and signaling molecules are recruited. Thus activation of integrins affects signal cascades similar to those triggered by growth factor receptors[50, 51]. Focal adhesions function also as transmembrane structural links between the extracellular matrix and cytoskeleton inside the cell and affect its organization. They provide anchorage signal and all these structures directly support migration, cell cycle progression and expression of differentiation-related genes[52]. Actin cytoskeleton and focal adhesion protein vinculin have shown significant differences between cells grown on the non-treated and plasma treated samples. Especially in MSC and DPC cells on He-APGD treated disks the actin stress fibers emerged earlier, were thicker, longer, and reinforcing the lamellipodia-like projections of cell membrane. These fibers were ended with well defined, vinculin-

positive focal adhesions. In contrast cells on non-treated samples had visibly inferior level of cytoskeleton and focal adhesion organization, actin and vinculin were both found in a rather undefined diffuse form in cell cytoplasm. Enhanced vinculin expression in MSC cells on He-APGD treated disks 12 hr after cell seeding was confirmed also by western blot analysis. Similar observations were reported also on UV-functionalized[13, 27] or vacuum glow discharge treated titanium[21].

This slower rate of spreading could affect the subsequent proliferative activity[53, 54]. Cells with lower adhesion area and round shape were found to have also lower rates of proliferation. It has even been suggested that a prolonged period in a round cell shape triggers a pattern of gene activation that is comparable with that expressed during cell growth arrest[55]. Similar trend was also observed on the He-APGD treated titanium. Cells growing on plasma treated disks that had larger attachment area also showed significantly higher proliferation rates.

As it was mentioned above, cell initial attachment and spreading can influence also signaling cascades regulating differentiation of osteoblasts. In this respect $alpha_V$ integrins may play an important role in signaling and osteoblast differentiation by interacting with growth factor receptors[50]. After the initial attachment osteoblast progenitor cells go through successive developmental stages, starting with proliferation, followed by bone matrix formation/maturation phase, characterized by alkaline phosphatase upregulation and ECM protein expression, and finished by mineralization stage, during which the bone matrix is mineralized by calcium phosphate deposits[56]. Dental pulp cells are adult stem cells capable of differentiation into osteoblasts upon stimulation with osteogenic media.

He-APGD treatment showed no significant effect on ALP expression in these cells. This is in contrast with the results from the UV-activated titanium, which has been shown to stimulate osteogenic differentiation in mesenchymal stem cells[27]. However, as it was mentioned, alkaline phosphatase is only an early marker of osteogenic differentiation and therefore further experiments examining late markers, such as expression of ECM proteins and matrix mineralization need to be performed to describe the effect of He-APGD treatment on differentiation of osteoprogenitor cells.

V. CONCLUSION

In conclusion, this study examined the possibility of using a novel kind of titanium surface treatment with helium atmospheric pressure glow discharge to increase its bioactivity and thus improve the osseointegration of implants made from this material. It was demonstrated that He-APGD can be used for effective surface modification of titanium. The treatment created a superhydrophilic surface within a short treatment time and with a relatively strong resistance to recovery. The modification enhanced significantly initial cellular response, such as cell attachment, spreading and proliferation in three different types of osteoblast progenitor cells. Although the exact mechanism of this effect remains unknown, based on the obtained data it was suggested that hydrocarbon contaminant removal, hydroxyl group grafting and partially also changes in surface roughness created superior surface for increased adsorption of fibronectin, a protein of critical importance for cell/biomaterial interaction. The improved cell response seems to be therefore a result of fibronectin-integrin mechanism.

REFERENCES

1. Liu XY, Chu PK, Ding CX. Surface modification of titanium, titanium alloys, and related materials for biomedical applications. Materials Science and Engineering 2004; 49–121.
2. Ellingsen JE, Thomsen P, Lyngstadaas SP. Advances in dental implant materials and tissue regeneration. Periodontology 2000 2006;41:136–56.
3. Lench LL, Polak JM. Third generation biomedical materials. Science 2002;295:1014–7.
4. Albrektsson T, Johansson C. Osteoinduction, osteoconduction and osseointegration. Eur Spine J 2001;10: 96–101.
5. Kasemo B, Lausmaa J. Material-tissue interfaces: The role of surface properties and processes. Environ Health Perspect 1994;102(Suppl 5):41–5.
6. Guehennec LL, Soueidan A, Layrolle P, Amouriq Y. Surface treatments of titanium dental implants for rapid osseointegration. Dental Materials 2007;23: 844–54.
7. Lim YW, Kwon SY, Sun DH, Kim HE, Kim YS. Enhanced cell integration to titanium alloy by surface treatment with microarc oxidation. Clin Orthop Relat Res 2009;467: 2251–8.
8. Gupta A, Dhanraj M, Sigavami G. Implant surface modification: review of literature. The Internet Journal of Dental Science 2009;7.

9. Wall I, Donos N, Carqvist K, Jones F, Brett P. Modified titanium surfaces promote accelerated osteogenic differentiation of mesenchymal stromal cells in vitro. Bone 2009;45:17–26.
10. Molenberg A, Schwarz F, Herten M, Berner S, de Wild M, Wieland M. Improved osseointegration of a novel, hydrophilic Ti surface – a review. Materialwissenschaft und Werkstofftechnik 2008;40(1–2):31–5.
11. Schwarz F, Wieland M, Schwartz Z, Zhao G, Rupp F, Geis-Gerstorfer J et al. Potential of chemically modified hydrophilic surface characteristics to support tissue integration of titanium dental implants. J Biomed Mat Res B: Appl Biomater 2009;88B:544–57.
12. Aita H, Hori N, Takeuchi M, Suzuki T, Yamada M, Anpo M et al. The effect of ultraviolet functionalization of titanium on integration with bone. Biomaterials 2009;30:1015–25.
13. Iwasa F, Hori N, Ueno T, Minamikawa H, Yamada M, Ogawa T. Enhancement of osteoblast adhesion to UV-photofunctionalized titanium via an electrostatic mechanism. Biomaterials 2010;31:2717–27.
14. Poncin-Epaillard F, Legeay G. Surface engineering of biomaterials with plasma techniques. J Biomater Sci Polymer Ed 2003;10:1005–28.
15. Teraoka F, Nakagawa M, Hara M. Surface modification of poly (L-lactide) by atmospheric pressure plasma treatment and cell response. Dental Materials Journal 2006;5(3)560–5.

16. Khang G, Lee SJ, Lee JH, Kim YS, Lee HB. Interaction of fibroblast cells on poly(lactide-co-glycolide) surface with wettability chemogradient. Bio-Medical Materials and Engineering 1999;9:179–87.
17. Shenton MJ, Stevens GC. Surface modification of polymer surfaces: atmospheric plasma versus vacuum plasma treatments. J Phys d: Appl Phys 2001;34:2761–8.
18. Bardos L and Barankova H. Plasma processes at atmospheric and low pressures. Vacuum 2009;83:522–7.
19. Lin CC, Cheng HC, Huang CF, Lin CT, Lee SY, Chen CS et al. Enhancement of biocompatibility on bioactive titanium surface by low-temperature plasma treatment. Japanese Journal of Applied Physics 2005;44(12):8590–8.
20. Yamamoto H, Shibata Y, Miyazaki T. Anode glow discharge plasma treatment of titanium plates facilitates adsorption of extracellular matrix proteins to the plates. J Dent Res 2005;84(7):668–71.
21. Shibata Y, Hosaka M, Kawai H, Miyazaki T. Glow discharge plasma treatment of titanium plates enhances adhesion of osteoblast-like cells to the plates through the integrin-mediated mechanism. Int J Oral Maxillofax Implants 2002;17:771–7.
22. Han IH, Baik HK, Shin SW, Lee IS. Activated calcium silicate thin film by He plasma treatments. Surf Coat Tech 2008;202,5746–9.

23. Vandrovcova M, Vacik J, Svorcik V, Slepicka P, Kasalkova N, Vorlicek V et al. Fullerene C60 and hybrid C60/Ti films as substrates for adhesion and growth of bone cells. Phys Stat Sol(a) 2008;205(9):2252–61.

24. Vohra S, Hennessy KM, Sawyer AA, Zhuo Y, Bellis SL. Comparison of mesenchymal stem cell and osteosarcoma cell adhesion to hydroxyapatite. J Mater Sci: Mater Med 2008;19:3567–74.

25. Aronsson BO, Lausmaa J, Kasemo B. Glow discharge plasma treatment for surface cleaning and modification of metallic biomaterials. Journal of Biomedical Materials Research 1997;35:49–73.

26. Stanford CM, Keller JC, Solursh M. Bone cell expression on titanium surfaces is altered by sterilization treatments. J Dent Res 1994;73(5):1061–71.

27. Aita H, Att W, Ueno T, Yamada M, Hori N, Iwasa F et al. Ultraviolet light-mediated photofunctionalization of titanium to promote human mesenchymal stem cell migration, attachment, proliferation and differentiation. Acta Biomaterialia 2009;5:3247–57.

28. Aita H, Hori N, Takeuchi M, Suzuki T, Yamada M, Anpo M et al. The effect of ultraviolet functionalization of titanium on integration with bone. Biomaterials 2009;30:1015–25.

29. Bullock EL. Clean and hydroxylated rutile TiO_2 (110) surfaces studied by X-ray photoelectron spectroscopy. Surface Science 1996;352-354:504–10.

30. Du Y, Deskins NA, Zhang Z, Dohnalek Z, Dupuis M, Lyubinetsky I. Two pathways for water interaction with oxygen adatoms on TiO_2 (110). Physical Review Letters 2009;102:096102.
31. Wendt S, Schaub R, Matthiesen J, Vestergaard EK, Wahlström E, Rasmussen ED et al. Oxygen vacancies on TiO_2 (110) and their interaction with H_2O and O_2: A combined high-resolution STM and DFT study. Surface Science 2005;598:226–45.
32. Shultz AN, Jang WY, Hetherington WM, Baer DR, Wang LQ, Engelhard MH. Comparative second harmonic generation and X-ray photoelectron spectroscopy studies of the UV creation and O_2 healing of Ti^{3+} defects on (110) rutile TiO_2 surfaces. Surface Science 1995;339:114–24.
33. Lin CC, Cheng HC, Huang CF, Lin CT, Lee SY, Chen CS et al. Enhancement of biocompatibility on bioactive titanium surface by low-temperature plasma treatment. Japanese Journal of Applied Physics 2005;44(12):8590–8.
34. Tang S, Kwon OJ, Lu N , Choi HS. Surface characteristics of AISI 304L stainless steel after an atmospheric pressure plasma treatment. Surface & Coatings Technology 2005;195:298–306.
35. Cai L, Bossert J, Jandt KD. Does the nanometre scale topography of titanium influence protein adsorption and cell proliferation? Colloids and Surfaces B: Biointerfaces 2006;49:136–44.

36. Vagaska B, Bacakova L, Filova E, Balik K. Osteogenic cells on bio-inspired materials for bone tissue engineering. Physiological research 2010;ahead of publication.
37. He J, Zhou W, Zhou X, Zhong X, Zhang X, Wan P et al. The anatase phase of nanotopography titania plays an important role on osteoblast cell morphology and proliferation. J Mater Sci: Mater Med 2008;19:3465–72.
38. de Oliveira PT, Nanci A. Nanotexturing of titanium-based surfaces upregulates expression of bone sialoprotein and osteopontin by cultured osteogenic cells. Biomaterials 2004;25:403–13.
39. Webster TJ, Ejiofor JU. Increased osteoblast adhesion on nanophase metals: Ti, Ti6Al4V, and CoCrMo. Biomaterials 2004;25:4731–9.
40. Biggs MJP, Richards RG, Dalby MJ. Nanotopographical modification: a regulator of cellular function through focal adhesions. Nanomedicine: Nanotechnology, Biology, and Medicine 2010; ahead of publication.
41. Thomas CH, McFarland CD, Jenkins ML, Rezania A, Steele JG, Healy KE. The role of vitronectin in the attachment and spatial distribution of bone derived cells on materials with patterned surface chemistry. J Biomed Mater Res 1997;37:81–93.
42. Horbett TA. The role of adsorbed proteins in tissue response to biomaterials. In: Hoffman AS, Schoen FJ, Lemons JE, Ratner BD, editors. Biomaterials science: an introduction to materials in medicine. 2nd ed. Amsterdam, Elsevier Academic Press; 2004. p.237–46.

43. Pegueroles M, Aparicio C, Bosio M, Engel M, Gil FJ, Planell JA et al. Spatial organization of osteoblast fibronectin matrix on titanium surfaces: Effects of roughness, chemical heterogeneity and surface energy. Acta Biomaterialia 2010;6:291–301.

44. Globus RK, Doty SB, Lull JC, Holmuhamedov E, Humphries MJ, Damsky CH. Fibronectin is a survival factor for differentiated osteoblasts. J Cell Sci 1998;111:1385–93.

45. Velling T, Risteli J, Wennerberg K, Mosher DF, Johansson S. Polymerization of type I and III collagens is dependent on fibronectin and enhanced by integrins alpha(11)beta(1) and alpha(2)beta(1). J Biol Chem 2002;277:37377–81.

46. Anselme K. Osteoblast adhesion on biomaterials. Biomaterials 2000;21:667–81.

47. Sousa SR, Lamghari M, Sampaio P, Moradas-Ferreira P, Barbosa MA. Osteoblast adhesion and morphology on TiO_2 depends on the competitive preadsorption of albumin and fibronectin. J Biomed Mater Res 2008;84A:281–90.

48. Grinnell F, Feld MK. Initial adhesion of human fibroblasts in serum-free medium: possible role of secreted fibronectin. Cell 1979;17:117–29.

49. Hynes RO. Integrins: Bidirectional, allosteric signaling machines. Cell 2002;110: 673–87.

50. Lai CF, Cheng SL. αvβ integrins play an essential role in BMP-2 induction of osteoblast differentiation. J Bone Miner Res 2005;20:330–40.

51. Garcia JA. Get a grip: integrins in cell-biomaterial interactions. Biomaterials 2005;26:7525–9.

52. Danen EHJ, Sonnenberg A. Integrins in regulation of tissue development and function. J Pathol 2003;200:471–80.

53. Uggeri J, Guizzardi S, Scandroglio R, Gatti R. Adhesion of human osteoblasts to titanium: A morpho-functional analysis with confocal microscopy. Micron 2010; 41(3):210–9.

54. Bacakova L, Filova E, Rypacek F, Svorcik V, Stary V. Cell adhesion on artificial materials for tissue engineering. Physiol Res 2004;53 Suppl 1:35–45.

55. Huang S, Ingberg DE. Shape-dependent control of cell growth, differentiation, and apoptosis: switching between attractors in cell regulatory networks. Experimental Cell Research 2000;261:91–103.

56. Choi JY, Lee BH, Song KB, Park RW, Kim IS, Sohn KY et al. Expression patterns of bone-related proteins during osteoblastic differentiation in MC3T3-El cells. Journal of Cellular Biochemistry 1996;61:609–18.